Enzymatic Activity and Excited State Processes in Protochlorophyllide Oxidoreductase

Sytina, O.

2010

~ CHAPTER 6 ~

Single and Multi-Exciton Dynamics of Protochlorophyllide Aggregates in Aqueous Solution

Olga A. Sytina, Ivo H. M. van Stokkum, Rienk van Grondelle and Marie Louise Groot

In plants, the oxidoreductase enzyme POR reduces protochlorophyllide into chlorophyllide, using NADPH as a cofactor. The reduction involves the transfer of two electrons and two protons to the C17=C18 double bond of Pchlide, and the reaction is initiated by the absorption of light by Pchlide itself[20, 52]. In this work the results of ultrafast time-resolved transient absorption and fluorescence experiments performed on protochlorophyllide in aqueous solution in the 480-720 nm visible region and in the 1780-1600 cm^{-1} mid-IR region are presented. Pchlide dissolved in water forms aggregates in which excitonic interactions dominate the optical properties. The ground state visible absorption spectrum of aqueous Pchlide red shifts and broadens if compared to the spectrum of monomeric Pchlide in organic solvents. In the excited state the population of the one-exciton state occurs at excitation densities with 1 photon per aggregate, at higher densities subsequent population of multi-exciton manifolds is observed. The multi-exciton state is characterized by blue-shifted stimulated emission and red-shifted excited state absorption in comparison to those of the one-exciton manifold. The relaxation dynamics of the multi-exciton manifolds into the one-exciton manifold is found to occur in ~10 ps. It is suggested that this rate is slow, because of mixing of exciton states with charge-transfer states. Structural features of Pchlide water adduct states are discussed as well.

6.1. Introduction

Protochlorophyllide (Pchlide) is a natural porphyrin, a precursor of chlorophyll *a* that is synthesized by plants for its photosynthetic apparatus. Natural porphyrins perform important functions in biology, for example, they participate in electron and excitation energy transfer processes in photosynthesis[114]; in oxygen transport and storage[115]; and function as catalytic centers[5, 20, 52]. Assemblies of (bacterio-)chlorophyll porphyrins play an important role in photosynthesis and porphyrin molecules may have potential uses as nonlinear optical materials and in artificial photosynthesis[116]. Self-aggregation of porphyrins and their analogues has been known to affect their optical absorption and emission properties.

Generally, when two identical molecules come in to close proximity of each other, their interacting transition dipole moments create a system of coupled electronic transitions. This so-called exciton coupling, is in the case of porhyrins facilitated by the conjugated electron system via π–π stacking. Excitonic coupling causes a splitting of the electronic energy levels of individual molecules into a manifold of excitonic levels. The splitting between the exciton levels is determined by the coupling strength, while the mutual orientation of the dipole moments of the coupled molecules (parallel *vs.* antiparallel) determines the oscillator strength of the levels, i.e. to which extend the transition is optically allowed[117, 118]. The amplitude of splitting is determined by the dipole-dipole interaction energy[119]:

$$V_{d-d} = \frac{|\mu 1| \cdot |\mu 1|}{4\pi\varepsilon_0 R^3}\left((\vec{r}1 \cdot \vec{r}2) - 3(\vec{r}1 \cdot \vec{R})(\vec{r}2 \cdot \vec{R})\right)$$

where magnitudes of the transition dipoles are $|\mu 1|$ and $|\mu 2|$; $\vec{r}1$ and $\vec{r}2$ are unit vectors in the directions of the transition dipoles; $\vec{R}$ is a unit vector connecting the centers of the transition moments; the scalar *R* is the center-to-center separation between dipoles; ε_0 is the dielectric constant. Calculating the scalar products for different mutual dipole orientations one can get the schematic energy diagrams as shown in figure 6.1. So-called H-aggregates, in which two molecules are oriented in parallel, show a blue shift of the electronic absorption relatively to the monomer absorption band, whereas J-aggregates in which molecules are oriented anti-parallel demonstrate a red shift in the electronic absorption spectra[120, 121].

The optical properties of Pchlide are determined by the mutual structural organization of solute and solvent. For example, protochlorophyllide dissolved in the organic solvent tetrahydrofuran (THF) or methanol (MeOH) has its Q_Y transition at 628-630 nm, but the Q_Y band experiences a strong shift to 650-654 nm when Pchlide is

dissolved in neat water. The effect is illustrated in figure 6.2.A. It is known that chlorophyll *a* displays a very unusual absorption and emission spectrum in aqueous solution: the Q_Y band experiences a dramatic shift from 663 nm to 747 nm and the yield of chlorophyll fluorescence in wet organic solution is found to be inversely proportional to the molar fraction of water[95, 122]. The alteration of the optical properties in aqueous solution is due to the formation of aggregates and chlorophyll–water adduct states, and the resulting excitonic interactions within the aggregate. Early on, large efforts have been applied to investigate the structure of chlorophyll aggregates both by experimental techniques and theoretically, because of their relevance to the organization of the pigments that constitute the electron donors in reaction center proteins of photosynthetic bacteria and green plants in Photosystem I[122-125], and for the organization of the bacteriochlorophyll pigments in chlorosomes[126, 127]. For chlorophyll-water aggregates, polarized spectroscopy and neutron diffraction suggest a long tube-like structure of the aggregates[128, 129]. Applying quantum chemical calculations to a one dimensional chlorophyll-water aggregate, Linnanto *et al*[129] modeled a helical structure with a circular diameter of 12 nm, close to the experimentally observed diameter of 11.4 nm of the aggregates in solution. Typically, the aggregates consisted of 38 molecules. Nevertheless, no ultrafast time-resolved spectroscopy on chlorophyll *a* in aqueous solution has been performed to characterize the dynamics within these aggregates, besides the work of Helenius *et al*[130, 131], using a single-color transient absorption technique.

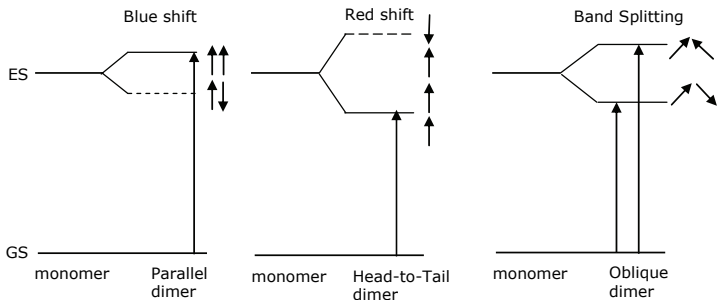

Figure 6.1. Illustration of the basic principle of excitonic interaction in a homodimer. In simplistic terms, parallel dipoles repel each other and create a higher energy state, while the antiparallel dipoles attract, which lowers the energy. Therefore the head-to-tail geometry creates a red-shifted transition, whereas parallel geometry creates a blue-shifted transition. In the case of oblique geometry of the transition dipole moments there is a band splitting into red and blue-shifted transitions. In terms of excitonic theory for the excitonically coupled dimer the two excitonic transitions acquire a different dipole strength, dependent on the structure of the dimer. ES on the scheme is supposed to be a one-exciton manifold or state, higher excitonic excited states are located above it. The one-exciton state (ES) in the diagram splits into lower and upper exciton levels.

In this work we present the results of ultrafast time-resolved transient absorption and fluorescence experiments performed on protochlorophyllide in aqueous solution in the 480-720 nm visible region and in the 1780-1600 cm^{-1} mid-IR region. In plants, the oxidoreductase enzyme POR reduces protochlorophyllide into chlorophyllide, using NADPH as a cofactor. The reduction involves the transfer of two electrons and two protons to the C17=C18 double bond of Pchlide, and the reaction is initiated by the absorption of light by Pchlide itself[20, 52]. The intrinsic reactivity of Pchlide in the excited state will be relevant also for the dynamics of Pchlide dissolved in water. In fact, it was shown theoretically by Zhao *et al*[41] that the Pchlide excited state has internal charge-transfer character which leads to a strengthening of H-bonding interaction, and results in a red shift of absorption and emission bands. Therefore in this work we will consider jointly the effects of excitonic and H-bonding interactions as the main factors determining the optical properties of Pchlide in solution. Our data is also relevant for *in vivo* studies, where in etiolated leaves red-absorbing aggregates of Pchlide have been observed, of which the role in the catalytic mechanism has remained unclear so far.

6.2. Materials and Methods

Protochlorophyllide was extracted from *Rhodobacter capsulatus* ZY5 as is described previously by Heyes [38] and was dissolved in neat H_2O or D_2O (purchased from Merck) to an OD of ~0.2 at 650 nm in a 200 μm cell.

Visible transient absorption measurements were performed by pumping the red edge of the Soret transition of Pchlide at 475 nm with a 85 fs laser pulse, and monitoring the resulting absorption changes in the region of the Q_X and Q_Y electronic transitions by a 480-720 nm white-light probe beam. After passing the sample cell, the probe beam was dispersed in a 2-nm resolution spectrograph and imaged on to a 256-element diode array. The instrument response function of the setup was about 120 fs, and the experiments were performed at a 1 kHz repetition rate. Transient absorption mid-IR spectra were measured on the same setup[67, 132] in the 1580-1800 cm^{-1} region using 400-nm excitation. In both experiments the pump beam was sent over a moveable delay line, enabling the measurement of absorption difference spectra at time delays from -15 ps to 5.5 ns. The excitation energy per pulse was adjusted by a neutral density filter to between 10 nJ up to 430 nJ in the vis-vis experiments, and 500 nJ in the mid-IR-vis experiment and focused into a 160 μm diameter spot.

Time-resolved fluorescence was collected in the region 450-750 nm using a synchroscan streak camera Hamamatsu C5680, upon 400 nm excitation with a 50 fs laser pulse at a 250 kHz repetition rate. The instrument-response function of this setup was

estimated to be ~3.5 ps for measurements performed in a 200 ps time window. The excitation energy in the experiment was 1 nJ per laser pulse. The setup and fitting methods are described in more detail by van Stokkum *et al* [87].

In every experiment the relative polarizations of the pump and probe light were oriented at the magic angle (54.7°). For the time-resolved fluorescence measurements a stirred 1 cm quartz cell was used, for the time-resolved transient absorption measurements a 200 μm path cell was used, with CaF_2 windows. The latter was built into a Lissajous sample scanner which allowed to collect the signal from a fresh sample spot for each laser shot.

Steady-state visible absorption spectra were recorded using a Perkin Elmer Lambda 40UV/VIS spectrograph, steady-state fluorescence spectra were collected by a Fluorolog FL-1039 apparatus, upon excitation at 400 nm through a 1 nm wide filter.

6.3. Results

6.3.1. Steady-State Absorption and Emission Spectra

Absorption and fluorescence emission spectra of Pchlide dissolved in 100% H_2O are depicted in figure 6.2.A. The positions of the S2 and S1 absorption bands of Pchlide in neat water are at significantly red-shifted positions in comparison to Pchlide in an organic solvent like THF (blue spectrum in figure 6.2.A). In aqueous solution the Q_Y maximum is between 650 nm and 654 nm, depending on the Pchlide concentration, whereas in THF it is at 629 nm. In the Soret region, the position of the main peak shifts from 444 to 480 nm. The emission spectrum of Pchlide in H_2O has a badly defined shape and basically consists of a broad signal extending from 600 nm to 700 nm with a peak at 650-660 nm (black line in figure 6.2.A). The intensity of the fluorescence emission was about 300 times weaker than that of Pchlide in organic solvents (figure 6.2.A, black line, signal is normalized to the absorption maximum of Q_Y). We observed no difference between the steady-state absorption spectra of Pchlide in H_2O and D_2O, besides minor variation in peak positions, which mainly depend on the concentration of the pigment in a particular sample preparation.

Addition of a few droplets of pyridine or THF into the Pchlide aqueous solution leads to a gain and blue shift of the Q_Y emission intensity. With a deconvolution analysis of the Q_Y band of the water-pyridine-Pchlide and water-THF-Pchlide mixtures, we could disentangle a red and a blue population (figure 6.2.C, D).

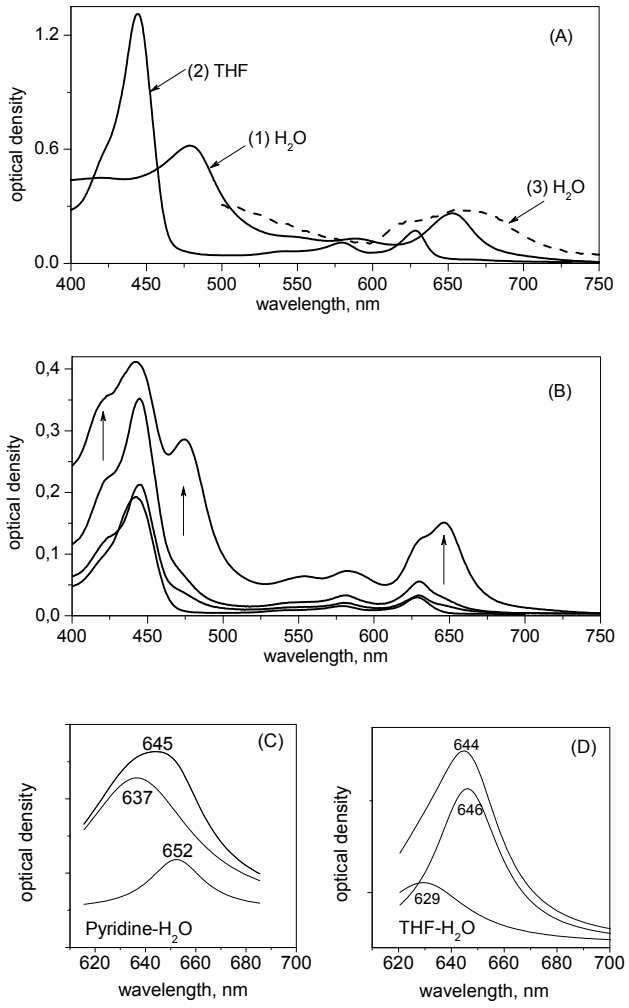

Figure 6.2. Absorption and emission spectra of Pchlide. **(A)** 1 – Pchlide absorption in 100% neat water solution recorded in a 1 cm cuvette; 2 – Pchlide absorption in THF; 3 – normalized steady-state fluorescence emission with 400 nm excitation. **(B)** Pchlide absorption spectra in THF recorded in 200 μm CaF_2 cell at increasing concentration of pigment. New bands appearing upon concentration increase are indicated by arrows. **(C)** Lorentzian deconvolution of the Q_Y absorption band of Pchlide in H_2O containing a few droplets of pyridine and **(D)** THF.

The blue states are typical for dry solutions, whereas the red state is characteristic for a wet solution. However, the red 646-nm state found in the water-Pchlide-THF mixture

can also be generated in dry THF upon increase of the pigment concentration. Figure 6.2.B demonstrates how a change in the relative concentration of THF solvent and pigment affects the steady-state spectrum of Pchlide. A typical low concentration spectrum of Pchlide dissolved in THF has peaks at 441 nm and 629 nm, increasing the Pchlide concentration leads to the appearance of new bands at 420 nm, 475 nm, 446 nm, and 646 nm. The positions of the new bands in the Soret are similar to those found in aqueous solutions. We also noted that a further 2-nm shift of the Q_Y absorption band towards the red can be forced by addition of base to the Pchlide water solution, i.e. with increase of OH^- concentration.

The significant redshifts of the absorption and emission spectra are indicative of the formation of aggregates of Pchlide, as similar effects have been observed for Chl in H_2O and have been shown to be caused by formation of aggregates and the resulting excitonic interactions[95, 128, 133, 134]. Also, our observation of reversible loss of Pchlide emission depending on solvent composition, is similar to observations reported for chlorophyll in water mixtures[95] and for Pchlide in aqueous methanol[113].

6.3.2. Time-Resolved Fluorescence

Time-resolved fluorescence decay traces of Pchlide in H_2O and D_2O were collected in the 500-750 nm region, in a 200 ps time window. The traces were analyzed globally with a sum of three sequentially decaying components; the results are shown in figure 6.3, in the form of evolution-associated spectra (EAS). The first EAS represents the spectrum directly after excitation, and has a main peak around 660 nm. After 2 ps, the intensity of the main band at 660 nm significantly diminishes but there is a small gain above 700 nm. This results in a double-peaked spectrum with a stronger emission at 690 nm rather than at 660 nm. A further decay of emission occurs in 7 ps and ~50 ps. The final spectrum with the 50 ps lifetime has a very badly defined shape because of its low intensity. The differences in emission spectra and lifetimes between H_2O and D_2O are likely due to slightly varying sample concentrations. The observed dynamics are dramatically different from those described previously in Chapter 5 for Pchlide in organic solvents. In water, the Pchlide fluorescence emission is virtually all quenched on a 2-7 ps time scale, and in conjunction with quenching, the emission shifts to lower energy. The latter may represent transfer of the excitation to sites of lower energy within an aggregate, and/or solvation processes.

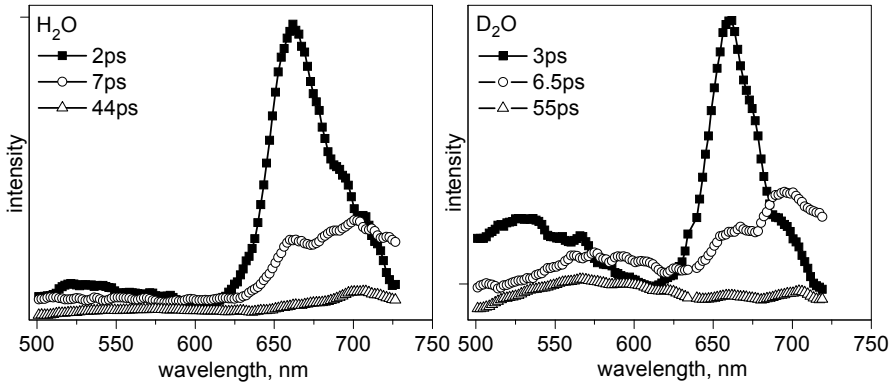

Figure 6.3. Evolution-associated spectra resulting from global analysis of the time-resolved fluorescence of Pchlide in H_2O (left panel) and Pchlide in D_2O (right panel) recorded upon 400 nm excitation with 1 nJ laser pulses.

6.3.3. Transient Absorption Spectra

To determine whether the emission is quenched due to a loss of excited states, or due to a decrease in the radiative rate, we performed transient absorption difference measurements. In addition, to test a possible power dependence of the kinetics, several excitation energies ranging from 10 nJ to 430 nJ per pulse were used.

All datasets were fitted with a sum of four sequentially decaying components, the lifetimes obtained at each excitation energy are shown in table 6.1. The first lifetime is sub-picosecond, ~0.5-0.6 ps; the second lifetime increases from ~2.3 ps to 8 ps; the third lifetime increases from 60 to 150 ps and the last increases from 1.5 ns to 3-4 ns. Negative bands in the corresponding EADS (figure 6.4) represent bleach of the ground state absorption and stimulated emission (SE), positive bands correspond to absorption from the excited state to higher lying electronic levels (ESA).

Low excitation energy

Similar to the fluorescence decay dynamics, the transient absorption (TA) dynamics demonstrate an ultrafast decay of broad difference signals. Comparing the 10 nJ TA dynamics with the fluorescence emission dynamics, which were recorded with an excitation

energy of 1 nJ per pulse, we see that in the TA about half of the signal is retained after ~ 2.3 ps, but the fluorescence emission virtually all decays on this time scale. This indicates that the initial loss of emission signal is not due to a loss of excited states, but to a reduction of the radiative rate, due to the formation of a 'dark' state with no or low transition dipole moment. Notably, as in the fluorescence experiment, this process occurs in conjunction with transfer of the excitation to sites of lower energy, since the pump-probe data show loss of relatively blue signal, between 640 and 660 nm, i.e. the recovery of blue, high-energy bleached absorption.

A further ~45% loss of the signal occurs with a time constant of 48 ps, in conjunction with a clear decay at the blue side of the difference spectrum, though no obvious shift in the 660 nm peak is observed.

High excitation energy

At excitation powers above 20 nJ per pulse, the initial decay accelerates: about half of the initial negative signal at 660 nm is lost after 0.5-0.7 ps (black to red evolution in figure 6.4). In addition, the initial EADS (black lines) show increased intensity at the high energy side, around 640-645 nm, with increasing excitation powers. This process goes along with a transition from negative to positive amplitudes in the 670-680 nm region. A comparison of selected time traces recorded at 20 nJ and 430 nJ illustrates this spectral change (figure 6.5.A, B, C). One can clearly see the dramatic difference in kinetics between the traces recorded at 644 nm and 675 nm, whereas the dynamics of the signals at 660 nm seem to be less affected upon 20-fold power increase. As we will show below and in more detail in the next chapter, this is a consequence of putting more than one photon in an Pchlide aggregate, which leads to the population of the two-, three- or higher-exciton manifolds, that apparently have different spectral features than the one-exciton manifold.

Table 6.1. Lifetimes obtained from the global analysis of the Pchlide in D_2O dataset recorded at different excitation energies per pulse, where applicable the rates in H_2O are reported as well.

Energy per pulse (nJ)	t1, ps (black)	t2, ps (red)	t3, ps (blue)	t4, ps (green)
10	0.5	2.3	48	1500
20	0.69	6.2	89	1900
40	0.49	5.5	83	1840
50 in H_2O	0.74	5.5	76	1500
60	0.49	4.3	46	1350
80	0.5	5.9	70	1630
100	0.56	7.2	96	3060
100 in H_2O	0.69	9.4	116	1580
130	0.62	9	126	2880
200	0.54	8.9	149	4100
200 in H_2O	0.62	11.2	178	1990
300 in H_2O	0.62	8.4	131	2430

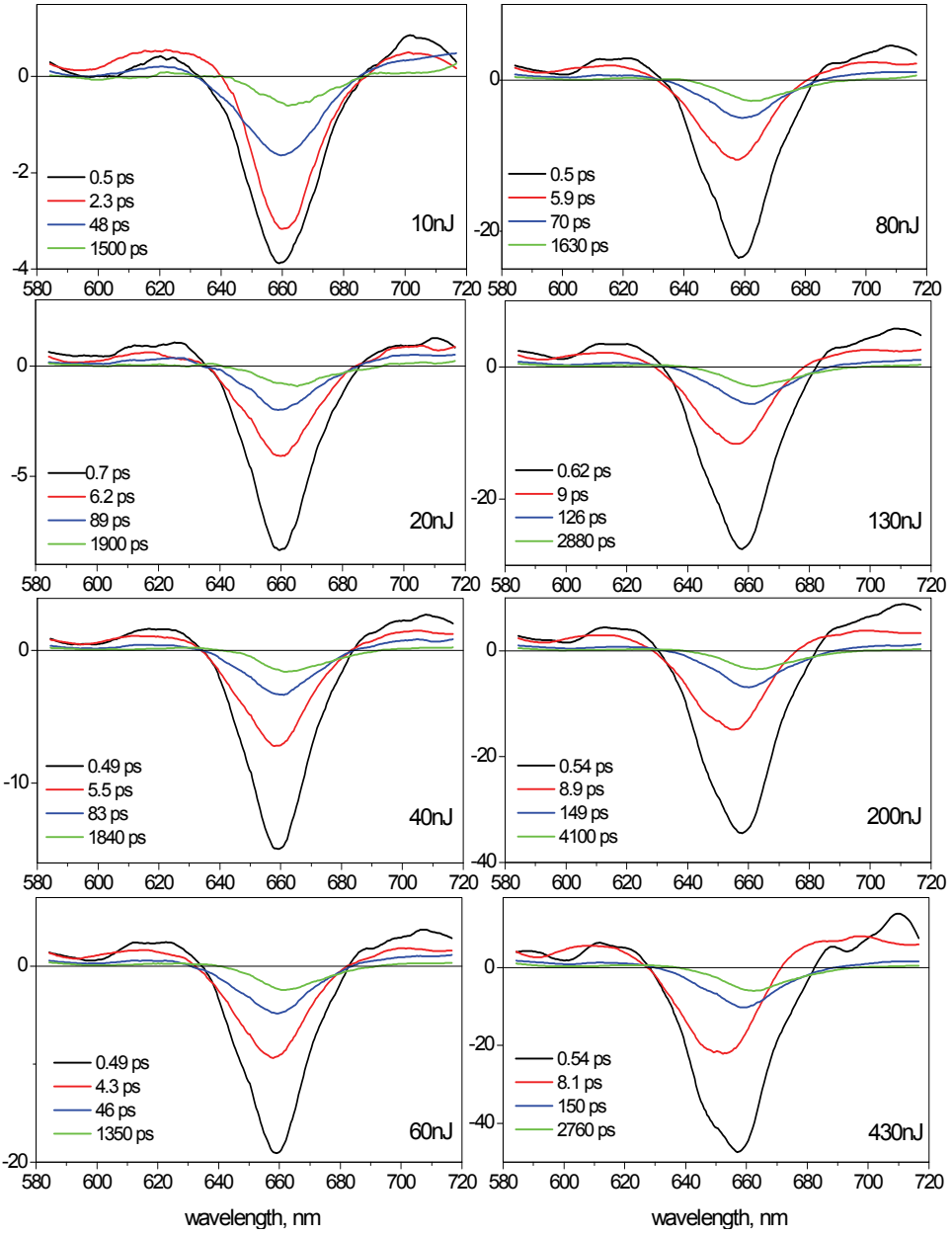

Figure 6.4. EADS resulting from global analysis of TA of Pchlide in D_2O excited at 475 nm with powers of 10, 20, 40, 60, 80, 130, 200, 430 nJ per laser pulse.

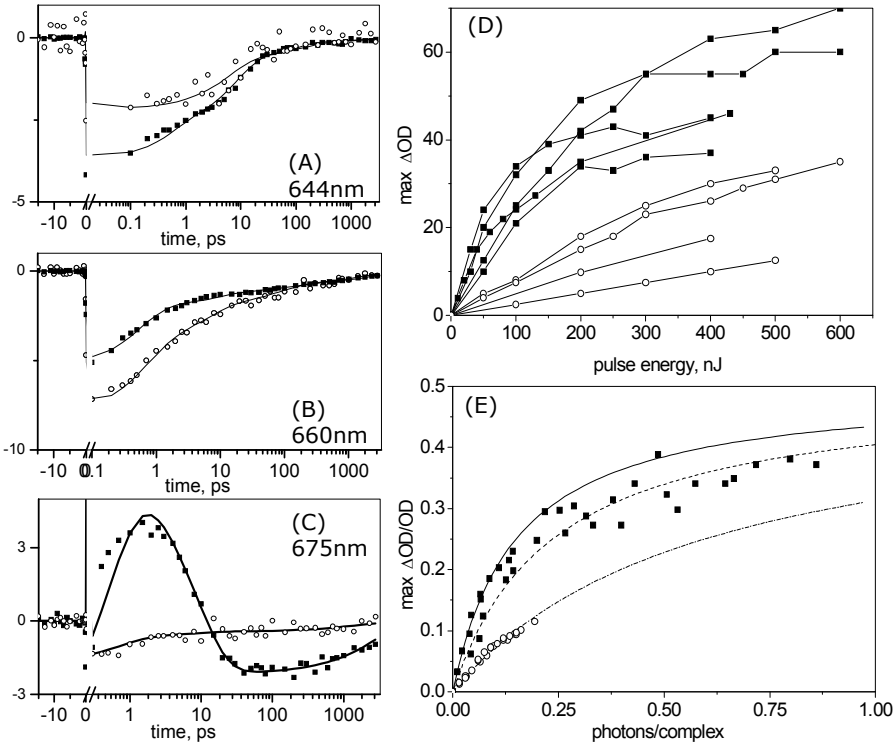

Figure 6.5. Traces of transient absorption of Pchlide in D_2O. Solid lines represent the fit, open circles – data points recorded with 20 nJ, black squares – data points recorded with 430 nJ excitation energy per pulse. **(A)** 430 nJ trace at 644 nm normalized to the amplitude of the 20 nJ signal at 1 ns delay. **(B)** 430 nJ trace at 660 nm normalized to the amplitude of the 20 nJ signal at 1 ns delay. **(C)** 675 nm traces without normalization. **(D)** Saturation of the transient absorption of Pchlide in different solvents as a function of excitation energy. Squares are measurements carried out in H_2O and D_2O, and open circles are measurements carried out in organic solvents (THF and methanol). The Y axis is the maximum amplitude of the negative signal 300 fs after excitation, in H_2O and D_2O it is at 655-660 nm, in organic solvents it is at 635 nm. **(E)** Corrected saturation of Pchlide transient absorption in water and organic solvents. The black squares are the experimental data averaged over five samples (3 in D_2O and 2 in H_2O), the open circles are experimental data in organic solvents averaged over 4 samples. On the Y axis the ratio of the integrated ΔmOD signal at t = 300 fs to the integrated absorption of the Q_Y band for each sample is plotted. The X scale is the excitation density recalculated to the number of photons per complex. The lines are saturation functions $F(N)=k\cdot N/Ns\cdot(1+ N/Ns)^{-1}$ fitted to the experimental data, with k=0.5, Ns=0.15 (black), Ns=0.22 (dashed), and Ns=0.6 (dash - dotted).

6.3.4. Saturation of the transient absorption signals

The size of the Pchlide aggregates determines at which excitation density the TA signals saturate. Therefore we can obtain an estimate of the aggregate size of Pchlide in water by plotting the relative TA signals as a function of excitation density per pigment, and calculating the saturation rate from the first order derivative of the saturation curves. As an internal check, we compare our results with those obtained for Pchlide in organic solvent for which we assume Pchlide to be in monomeric form.

The plots of the maximal ΔOD signal at t=0.3 ps after excitation, as a function of excitation energy, in different solvents (H_2O, D_2O, THF, and methanol) are shown in figure 6.5.D. Typically, the amplitude of the initial bleach of Pchlide in water right after excitation was a few times higher than that of Pchlide in organic solvents at the same excitation power at 475 nm, which is not only due to the higher OD of Pchlide in water at the wavelength of excitation (also 475 nm). The saturation curves in neat water explicitly demonstrate a non-linear behavior, whereas the curves obtained in organic solvents are linear functions of excitation power within the whole range of powers. The variation in amplitudes seen among different samples is due to variations in the concentration. The scatter can be partly eliminated if the Y-scale is converted into a relative change in absorption, and the X-scale into the number of absorbed photons per molecule. For this purpose the ΔmOD amplitudes were normalized to the optical density of the Q_Y band of each sample, thus making the experimental data independent on the sample preparation and variation of concentrations. The excitation energy was recalculated into the number of absorbed photons per molecule per pulse in each experiment, using the following expressions:

$$N_{photons} = \frac{E - E \cdot 10^{-ODex}}{E_{photon} \cdot S_f} \qquad (1)$$

$$N_{molecules} = \frac{N_A \cdot C(OD, \varepsilon, path) \cdot V}{S_f \cdot (1 - T)} \qquad (2)$$

where E is excitation energy in Joules; OD_{ex} is optical density at the excitation wavelength; E_{photon} is energy of one photon at the excitation wavelength; N_A is Avogadro number; $C(OD, \varepsilon, path) = \frac{OD}{\varepsilon \cdot path}$ is the concentration of the sample, which is a function of the optical density and extinction coefficient at the detection wavelength either 650 nm for Pchlide in water, or 630 nm for Pchlide in organic solvents, and path length of the sample cell; V is the volume of the sample illuminated by each laser shot;

$$S_f \cdot (1 - T) = S_f \cdot (1 - 10^{-ODex}) \qquad (3)$$

is the factor accounting for area covered by absorbing pigments, Sf was 160 μm, and cell path length was 200 μm.

The extinction coefficient of Pchlide in several organic solvents is known from the literature[7, 59], in this work we used ε = 30.4(10^{-3}M·cm)$^{-1}$ at 630-640 nm. Since we could find no report of the extinction coefficient of Pchlide in aqueous media in the literature, we determined the concentration using the assumption that the integral oscillator strength does not change in different media: F (in THF) ≅ F (in water). The oscillator strength is related to the extinction coefficient through the following expression:

$$F \cong 4.3 \cdot 10^{-9} \int \varepsilon \cdot d\lambda$$

Thus, the integral of the extinction coefficient in THF is identical to the one in water: $\int \varepsilon \cdot d\lambda$ (in THF) ≅ $\int \varepsilon \cdot d\lambda$ (in water).

Remembering that

$$\int \varepsilon \cdot d\lambda = \frac{\int OD \cdot d\lambda}{C \cdot path} \qquad (4)$$

we can determine the concentration of Pchlide in water relative to the concentration in THF. In this way we can convert the excitation energy per pulse into excitation density, i.e. number of photons per molecule for both aggregates and monomers. The final corrected curves are shown in the figure 6.5.E, where a clear difference between aggregate and monomer absorption saturation is seen. The different saturation measurements in THF and methanol now nicely coincide on one line, whereas the five measurements in H_2O and D_2O still show some scattering behavior. Possibly, this again reflects small differences in concentrations and aggregation sizes.

The experimental saturation curves can be fitted by the function:

$$f(N) = k \frac{\frac{N}{Ns}}{1 + \frac{N}{Ns}} \qquad (5)$$

where in this case N is excitation density, Ns is a saturation threshold, k=0.5 is a scaling coefficient accounting for the saturation effect of the SE (due to the fact that the Einstein coefficients of absorption and emission are equal). The derivative of this function is

$$\frac{df(N)}{dN} = k \frac{Ns}{(N + Ns)^2} \qquad (6)$$

from which we directly see that the derivative at zero is k/Ns photons per molecule.

Applying formula (5) to the experimental data we find that the data in water and organic solvents can be simultaneously best fitted when the ratio of the saturation

thresholds, Ns, of monomers to aggregates lies between 2.7 and 4. Therefore we conclude that the Pchlide aggregate domain size in neat water is on average 3-4, but there might be some variation in this number. Also, at lower concentrations there is likely to be an equilibrium or distribution of different domain sizes, perhaps varying between 2 and 4, since the red shift of the Q_Y band due to excitonic interactions is directly proportional to the pigment concentration. The structural features of aggregates will be discussed in more detail later in the chapter.

We note that the saturation threshold Ns in THF and methanol solutions was determined to be close to 0.6 photons per complex. However for a two level scheme it should be 0.5 photons per complex (i.e. 1 photon per 2 complexes) to obtain equilibrium between excited and ground state populations in a system consisting of 2 molecules. The discrepancy between expected and fitted values originates from the fact that the amplitude of the TA signals was registered at t= 0.3 ps, whereas a further gain of about 10% of the negative signal occurs in THF and methanol solutions on a timescale of a few ps, when excitation in the Soret is used. More details on the Pchlide TA experiments in THF are presented in chapter 5, where we showed that the gain in Q_Y bleach and SE signal is most likely caused by slow S2 to S1 relaxation and vibrational cooling. Therefore, if the amplitude of the TA signal had been registered at later delay times, it would have resulted in a steeper slope of the monomer saturation curve and yielded a threshold of 0.5 photons per complex.

6.3.5. Describing the saturation dynamics in a target model

From the time-dependent absorption saturation measurements and their global analysis it is clear that Pchlide in aqueous solution demonstrates pronounced non-linear dependence on power. We disentangled the low-power and high-power contributions by applying a target analysis to the data, with the kinetic scheme as shown in figure 6.6.A. In this scheme there is the low power dynamics, with the sequential formation in time of four states (1, 2, 3, 4), and an additional pathway, with two compartments 5 and 6. In the analysis both states 1 and 5 can receive input, i.e. be excited, and their population is a free fitting parameter, also in parallel there is a contribution of a coherent artifact. Since states 5 and 6 describe a high-power, multi-excitation process, we connect state 6 at a certain point to the sequence (1, 2, 3, 4), which describes the single excitation dynamics, to account for annihilation of the multiple excitations. Because in the global analysis the major power-dependent spectral difference is observed in the first and second EADS, the most probable kinetic scheme should include a decay of compartments 6 either to states 3 or 4, or directly to the ground state in ~10 ps after excitation.

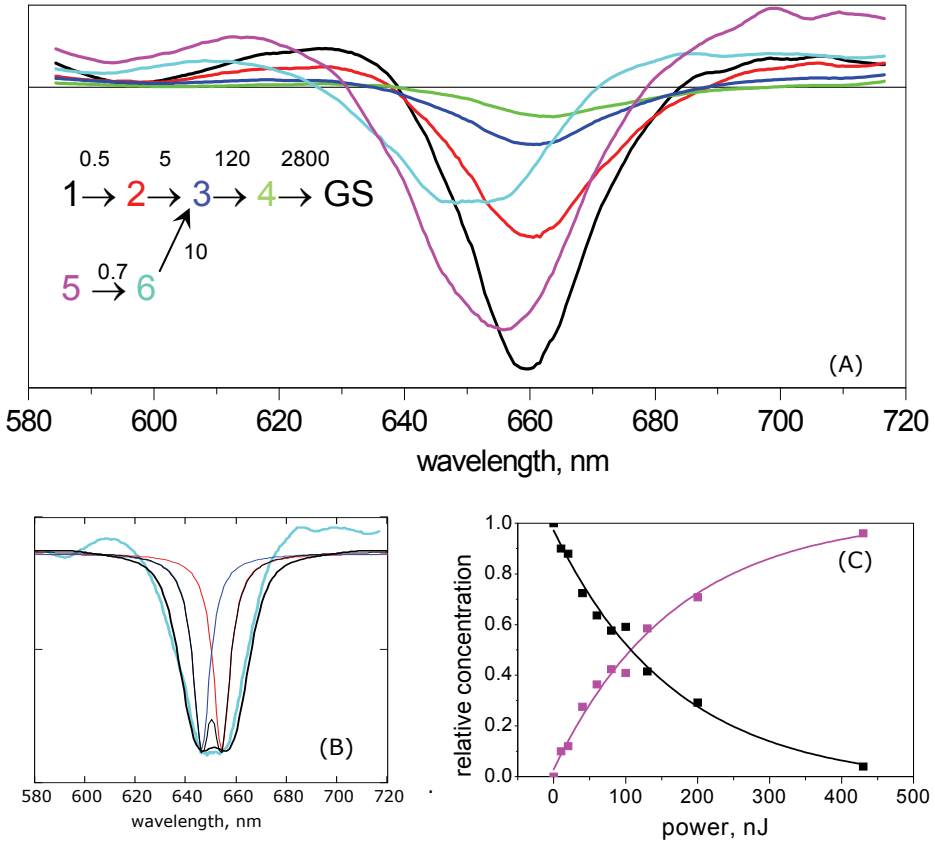

Figure 6.6. (A) Species-associated difference spectra obtained in target analysis in simultaneous fitting of transient absorption difference spectra recorded in solution of Pchlide in D_2O at different excitation powers. Black, red, blue and green lines are spectra of sequentially decaying compartments 1, 2, 3, and 4, Magenta and cyan spectra correspond to states 5 and 6; **(B)** Simulation of double-peaked spectrum (black line) with Voigt convolution of sum of two Lorentz lines at 645.5 nm (blue line) and 653.5 nm (red line) with broader Gaussian profile. Original spectrum from target analysis is represented by cyan line; **(C)** Black dots and exponential fit is the fraction of state 1 (one-exciton state) and, magenta dots and exponential fit is the fraction of state 5 (high-exciton state) as a function of excitation power.

The whole dataset consisting of nine individual measurements at different energies ranging from 10 nJ to 430 nJ per pulse was fitted simultaneously to this model and species–associated difference spectra (SADS) of each compartment, as well as their lifetimes and

fractions of the two schemes to the overall signal amplitude were estimated. The result of the target analysis and the kinetic scheme are depicted in figure 6.6.A. The black, red, blue and green SADS correspond to the sequentially decaying compartments 1, 2, 3, and 4, and magenta and cyan spectra correspond to compartments 5 and 6.

Upon increasing excitation density, the population of compartment 5 increases, and the population of compartment 1 decreases, resulting in the 5→6→3→4→GS kinetic scheme dominating at high excitation energies (figure 6.6.C). The contribution of the coherent artefact was negligible after 0.2 ps, and did not significantly affect the target analysis results, which take place on longer times. It appeared that the best separation of 'blue' and 'red' states was achieved in a model where the population of the non-linear branch decays into compartment 3 of the sequential scheme. When it decayed to the GS, a considerable portion of blue amplitudes was still present in the black and red spectra (not shown).

The evolution in the low-power compartments, loss of signal accompanied by a red shift of the signal, occurs with lifetimes of 0.5 ps, 5 ps, 120 ps and 2.8 ns. Only 10% of the initial amplitude is left in the final 2.8 ns-spectrum, and the bleaching maximum has shifted from 659 nm to 663-664 nm. The initial spectrum of the high-power dynamics (magenta) peaks at 656 nm and has a lifetime of 0.7 ps. The next spectrum (cyan) has a lifetime of 10 ps and a broadened double-peaked shape in the 625-670 nm region.

The signal between 670 and 720 nm signal is positive and flat; in this region there is a distinct power-dependent transition from negative to positive amplitudes together with gain in the blue side of Q_Y bleach (see the 675-nm time trace in figure 6.5.C). The double-peaked cyan spectrum can be well simulated by a Voigt profile composed of the sum of two Lorentzian spectral lines centered at 645.5 nm and 653.5 nm each convoluted with Gaussian. The simulated curve is overlaid on the SADS obtained from the target analysis in figure 6.6.B.

6.3.6. Time-resolved mid-IR spectroscopy

Transient absorption spectra between 1780 and 1660 cm^{-1}, in the region of the C=O 13^1 keto and 13^2 ester vibrations of Pchlide in neat D_2O, were collected to investigate the influence of H-bonding and aggregation behavior on the Pchlide excited state dynamics. In the mid-IR TA experiment a sample with an optical density similar to the one used in the visible experiments, i.e. about 0.2, was pumped in the Soret region at 400 nm with a laser power of ~500 nJ per pulse. The excitation power in the mid-IR TA experiment therefore corresponds to the saturating regime. The time-resolved data were globally fitted with a sum of four sequentially decaying exponential components of 0.6 ps, 4 ps, 80 ps and 2.3 ns.

The corresponding EADS are shown in figure 6.7, for comparison we refer to chapter 5, figure 5.5 for the EADS of Pchlide in organic solvents (THF, methanol). The lifetimes obtained in the global analysis of the mid-IR TA data are similar to the ones found for the visible TA data, at high power. Therefore, the final long-lived spectrum in the visible region can be associated with the final spectrum in the mid-IR region.

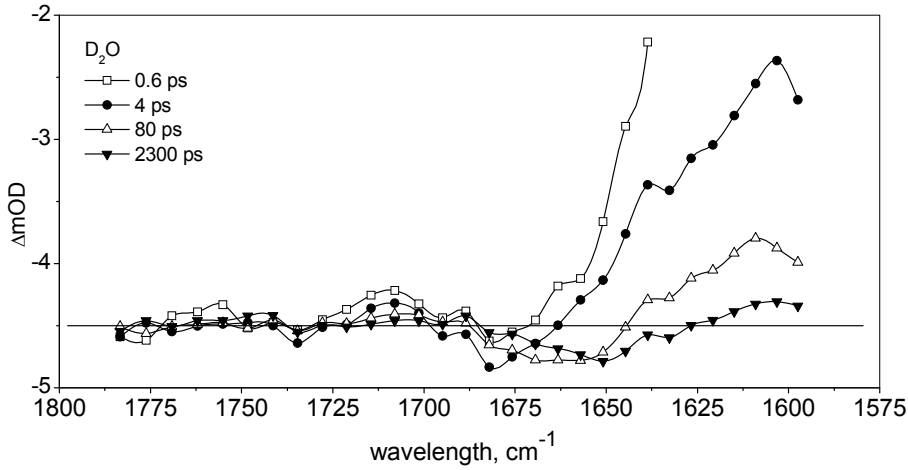

Figure 6.7. Evolution-associated difference spectra of time-resolved mid-IR transient absorption of Pchlide in D_2O upon 400 nm excitation.

The EADS of Pchlide in D_2O display multiple negative bands, presumably belonging to the C=O keto stretching vibrations. Negative peaks in the mid-IR transient absorption spectra belong to the bleached absorption of vibrations in the ground state and positive bands represent absorption due to the vibrations of the Pchlide molecule in the electronically excited state.

The spectra and dynamics observed in neat D_2O are remarkably different from those observed in the aprotic solvent THF, where the spectrum showed only a single keto mode. In the protic solvents methanol and water buffer solution (figure 5.5.B, C in chapter 5) two keto bands due to two subpopulations of pigments were observed. In neat D_2O the initial spectrum displays bleached ground state bands at 1680 cm^{-1}, a broad intense positive light-

induced band in the region below 1670 cm^{-1}, a small negative band at 1734 cm^{-1}, and positive signal between 1715-1690 cm^{-1}. The positive signal below 1670 cm^{-1} decays for a large part and redshifts in 0.6 ps, in conjunction with decay of the positive signal at 1704 cm^{-1} (black to red evolution in figure 6.7). The loss of the major part of the positive signal below 1670 cm^{-1} is accompanied by the appearance of negative bands at ~ 1666 and 1650 cm^{-1}. In 4 ps the initially bleached states at 1694 and 1680 recover and additional negative signals at 1650 cm^{-1} and 1634 cm^{-1} appear. We showed previously in chapter 5 that the keto vibration in monomeric and non H-bonded Pchlide in THF is located at 1708 cm^{-1} in the ground state and at 1660 cm^{-1} in the excited state; the position of the ester mode was found at 1750 cm^{-1} in the GS and at 1738 cm^{-1} in the ES. The present observation of a range of downshifted Pchlide keto-frequencies in neat water is an indication of the existence of several subpopulations of C=O keto groups with varying hydrogen bond strengths, either formed between subunits of an aggregate or with the surrounding solvent.

A correlation between the strength of hydrogen bonding and a shift of absorption bands towards longer wavelength in the visible region and lower wavenumbers as well in the IR regions has been established[41, 135]. The keto mode can coordinate to the magnesium atom of another pigment within the aggregate, via an OH bridge, or it can H-bond to the solvent, both lead to a downshift of the mode. The C=O stretching frequency downshifts with shortening of the C=O---H bond length, due to weakening of the covalent interaction in closer vicinity of the hydrogen atom. Using a formula for the harmonic oscillator we can roughly estimate that about 60-80% of extra deuterium mass should be present around the keto group to cause a shift of its vibration from 1680 cm^{-1} to 1650 cm^{-1} observed in our experiment. Therefore the low frequency keto modes can be an indication of intrinsic enol states in the aggregate. Tautomeric proton transfer in keto C=O to form enol C=O---H is known to cause a downshift of a carbonyl stretching frequency for many organic compounds, from the 1650-1750 cm^{-1} spectral window down to 1640-1580 cm^{-1} largely depending on the chemical compound and solvent[136, 137].

The recovery of high-energy bleached bands and the bleaching of lower frequency bands in time, can be linked to the observation of the red shift of the transient spectrum in the visible, and occurs with similar time constants. It shows that energy redistribution, either intra- or inter-aggregate, occurs on a ~10 ps time scale, from pigments with weak to pigments with strong hydrogen bonds.

6.4. Discussion

In this work we have used time-resolved visible and mid-IR spectroscopy to study the relation between the organization of the Pchlide chromophore and its spectral properties.

We find that Pchlide dissolved in neat water solution is characterized by (1) broadening and red shift of the steady-state absorption; (2) low steady-state emission signal; (3) loss of emission occurs with time constants of 3 ps, 7 ps and 50 ps; (4) at low excitation density the dynamics in the transient visible experiments occurs in 0.5 ps, 2.3 ps, 48 ps and 1.5 ns, at saturating excitation density these dynamics change into 0.5 ps, 8 ps, 150 ps and 2.8 ns, similar to the time constants obtained in the mid-IR (2 ps, 9 ps, 85 ps, 1.5 ns); (5) kinetic modeling of the visible TA data allows us to disentangle spectral features and dynamics typical for low excitation power and of high excitation power. In the following we will discuss several aspects of the interactions within the Pchlide aggregates and the resulting dynamics in more detail.

6.4.1. Dynamics in Pchlide aggregates

In section 6.3.4 we analyzed the different rates of saturation for the case of Pchlide in H_2O and Pchlide in THF and methanol. We find the ratio of the derivates of the saturation curves at zero excitatition energy to be ~3-4. Since we use here the transient absorption signals at t=0.3 ps, we measure in fact that the response upon absorption of a single photon induces a spectral change that is 3-4 larger for Pchlide in H_2O than in THF. This can be explained by excitonic interactions within aggregates of Pchlide, due to which the excitonic levels, within the one-exciton manifold, have a 3-4 times higher oscillator strength than of a monomeric Pchlide. From this we could conclude that the excitonic state involves 3-4 Pchlide molecules. However, we note that this is more likely a lower estimate of the aggregate size, since we measure a net absorption difference signal, and the population of a state within the one-exciton manifold may lead to more complicated, partially compensating, signals than bleaching of the ground state exciton absorption, and the stimulated emission from that state alone[138]. In chapter 7 we return to this issue when we calculate the absorption difference spectra of excitonically coupled Pchlide using exciton theory with a phenomenological line shape. Chlorophyll a in water has been computed by Linnanto *et al*[129] to form aggregates of about 40 to 90 molecules.

At the higher excitation densities, the transient spectra clearly show additional, negative and positive signals both at the high energy and the low energy side of the main band, respectively. Applying the target model depicted in figure 6.6.A, we could disentangle the low excitation energy and high-excitation energy dynamics and SADS. The low energy spectra and dynamics correspond to the dynamics within the one-exciton manifold, but the high-energy dynamics and SADS should be interpreted taking into consideration the multi-exciton manifold electronic transitions. To our knowledge, this is

the first clear demonstration of the population of multi-exciton manifolds for an aggregate in solution.

As an illustration of the special spectral signature of the multi-exciton manifold, let us assume that putting more photons into an aggregate induces correspondingly larger signals, which after annihilation processes result into the survival of one excitation per aggregate. Then this should result into a ratio of initial- to final- spectral area that is larger for the high-excitation energy case, than for the low-energy case. In contrast, we find a ratio of 99/14=7 for the 10 nJ and 1317/155=8.5 for the 430 nJ case. This illustrates that the premise that more photons per complex results in larger signals is largely wrong. Inspection of the SADS in figure 6.6.A confirms this, as the black spectrum is fairly similar in size to the magenta spectrum, and both finally feed into the green spectrum.

From exciton theory it is known that when N monomers form an aggregate, then the excited states are split into N excitonic manifolds, in which each manifold consists of N exciton levels, corresponding to different realizations of the wavefunction over the complex. In the TA saturation experiment we determined that the 430 nJ power exceeds 3-4 times the saturation threshold of the Pchlide aggregate (as can be derived using the method described in section 6.3.4 and also from comparison of the x scales in figure 6.5.D and 6.5.E). Upon absorption of one photon, the aggregate is promoted into the one-exciton state; with two, three and four photons it can be promoted to correspondingly higher exciton manifolds. In our analysis therefore we assign the sequential reaction 1-2-3-4 to dynamics of the lowest one-exciton state of the aggregate, whereas state 5, and 6, dominating at high excitation density, we assign to (an average of) higher exciton manifolds.

Since the initial population is divided between the two states 1 and 5, both SADS include the contribution from the bleached ground state absorption (GSB), apart from the contributions of stimulated emission (SE) and excited state absorption (ESA) to the relevant levels. In particular, the signal of SE in the sequential branch is due to the transition from the one-exciton state to the GS, therefore it is shifted to the red from the GS bleached absorption peak, whereas the SE in the magenta and cyan spectra is due to transitions from the higher exciton manifolds to lower exciton manifolds. In the simplest case, it is the transition from the two-exciton state to the one-exciton state. From the decomposition of the cyan SADS, we can see that the simulated 652 nm component is the GS bleach component, and the 645 nm simulated component is SE, suggesting that the multi-exciton SE covers a ~400 cm^{-1} higher energy difference than the GS to one-exciton absorption. The GS bleach component corresponds to the area formed by the overlap of the black (or red) and the cyan spectrum. In chapter 7 we will show that with exciton theory we can reproduce the one-exciton and multi-exciton difference spectra.

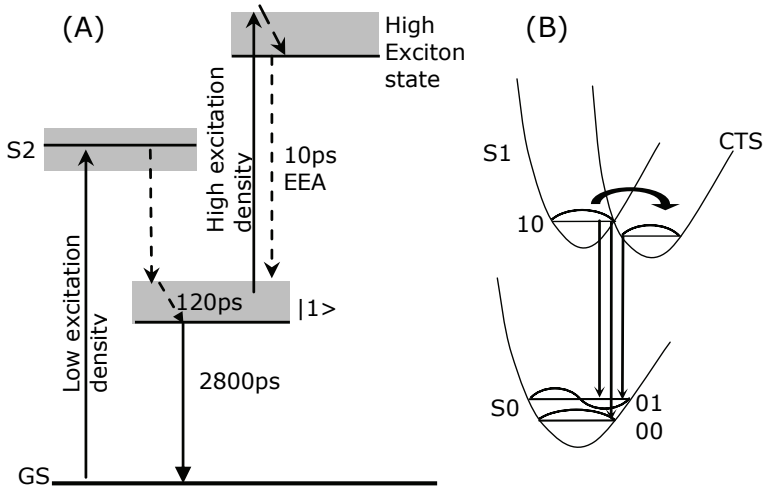

Figure 6.8. **(A)** Schematic energy diagram of the aggregated Pchlide in aqueous solution. Dashed arrows indicate a process of radiationless transitions, solid arrows indicate radiative transitions; **(B)** Mixing of charge-transfer state (CTS) with the S1 state. The transition to a coupled CTS potential leads to a reduced Frank-Condon overlap between the (1–0) excited state and the (0–0) GS levels, possibly the overlap between (1–0) and (0–1) is less affected, which then explains the time-resolved fluorescence dynamics.

We summarize the scheme of events upon excitation of the Pchlide aggregates in figure 6.8. After excitation in the Soret region at 475 nm the system undergoes fast radiationless internal conversion to the one-exciton state |1>, on S1. At high excitation density the aggregate can be promoted to the higher |2>, |3>, or |4>-exciton levels. For simplicity, in the diagram only the |2>-exciton level is depicted. From the target analysis we find that the population of the high exciton levels decays into the one-exciton manifold after 10 ps. This is surprisingly slow, in principle exciton-exciton annihilation should be a determining factor of the |2>, |3>, and |4>-exciton state decay, and usually exciton dynamics are assumed to occur rather on a sub-ps time scale[129, 139]. Two excitons spatially located within the same localization domain usually quickly annihilate, transferring their energy to an appropriate resonant monomer vibronic level. Possibly, in the Pchlide aggregates the intrinsic reactivity of the excited state is rate-limiting this process.

The dynamics within the one-exciton level occur on a time scale of 0.5 ps, 5 ps and 120 ps. From the fluorescence experiments in combination with the transient absorption experiments it is clear that the 0.5 and 5 ps represent the formation of a 'dark' state with no or low transition dipole moment, since the emission signal is almost totally lost, but the TA signal is only halved, indicating that the ground state absorption is not recovered. Such a dark state could be a state with significant charge-transfer (CT) character. It was demonstrated theoretically using time-dependent density functional theory (TDDFT) methods[41] that the red shift of Pchlide emission in the polar protic solvent methanol is due to a temporal strengthening of the site specific interaction between polar residues of Pchlide and OH-residues of methanol. Moreover, strengthening of the H-bonds facilitates the formation of charge-transfer states in the Pchlide excited state in methanol, because electron flow from the solvent to the Pchlide macrocycle and vice versa is coupled to hydrogen bond dynamics. The individual Pchlide S1 state was shown to intrinsically possess CT character as well[41] . Also for chlorophylls, it is known that the individual molecule possesses pronounced and a rather unusual combination of electron donor-acceptor properties. The keto C=O group of the cyclopentanone ring V can function as a donor, whereas the central Mg atom serves as an acceptor. Similarly, it was suggested by Zhao and Han[41] that in the electronically excited state of Pchlide, charge can be transferred from the Pchlide macrocycle to the cyclopentanone ring, in particular to the C=O keto group, as well as to the ethylene group at the site of C3. We suggest here, that the 0.5 and 5 ps dynamics of Pchlide in water are sequential solvation processes of this state, that result in strongly coordinated and hydrogen-bonded intermediates. We suggest in particular that the 0.5 ps and 5 ps processes occur in sequence, because the 0.5 ps CT formation may then be competitive with the intrinsic relaxation rate from the multi-exciton manifolds, resulting in CT formation on the exciton manifolds. Relaxation to the lower exciton manifolds would then first require the recombination from the CT state, slowing down the relaxation rate to $(10\ ps)^{-1}$. We will return to a discussion on the shape of the higher exciton manifold spectra and their dynamics in chapter 7.

Previously in time-resolved fluorescence and TA experiments carried out on Pchlide dissolved in methanol, we assigned the appearance of 646 nm red emission to formation of a state possessing a charge-transfer character. Recently the excited-state processes in Pchlide were studied using time-resolved fluorescence and pump-probe spectroscopy of Pchlide in several organic solvents (methanol, acetonitrile, hexane) in a 360 ps time window[84-86]. The experiments revealed Pchlide to be an intrinsically reactive molecule. The complex dynamics were interpreted with a model describing the excited-state processes in terms of a branching of the initially excited state population into a reactive and a non-reactive path. The reactive path entailed the formation of a state with intramolecular

charge-transfer character in 25 ps and subsequent decay in 200 ps; the non-reactive path displayed vibrational relaxation in 4 ps only.

6.4.2. Structure of Pchlide water adduct states

Pchlide is a pigment having a structure very similar to chlorophyll, therefore previous studies of chlorophyll a in aqueous solution provide an essential background for understanding the results obtained here. Chlorophyll *a* in wet organic solutions as well as in neat aqueous solution forms aggregates. A chlorophyll dimer or $(Chl - H_2O)_2$ water adduct state is considered to be the basic structural subunit where excitonic interaction is provided via stacking of two conjugated electronic clouds. In addition, for a long time chlorophyll *a* water adduct dimers have been a model for the optical properties of the special pair in PS1 photosynthetic complex, since there is a large resemblance of their visible absorptions. Initially, the model of a special pair of chlorophyll molecules for the electron donor in PS1 was proposed by Shipman and Katz[124]. A detailed review of chlorophyll water adduct states and aggregates can be found[122, 123, 140, 141]. Different possibilities of mutual chlorophyll and water organization have been discussed, but it has been shown that the fundamental and most essential characteristics in such a system is the coordination interaction between a pair of chlorophylls mediated by the OH group of an internal water molecule. Basically, the internal water molecule forms a bridge between the magnesium ion of one chlorophyll and the C=O keto group of another: Mg---H(OH)---O=C. Two water molecules can hold two pigments at a relative distance between the macrocycle planes of about 3Å, close to the optimal van der Waals distance for the porphyrins π-systems. The stacked dimer structure, with overlapping conjugated π-systems, leads to excitonic interaction, causing a red shift in the visible absorption spectrum. The most recent study of the chlorophyll *a* dimer organization was performed using atomic force microscopy[134], and the internal water molecule was found to be a key element responsible for the formation of chlorophyll a dimers.

We suppose that similar to chlorophyll, Pchlide in water forms dimers and oligomers coordinated by strong H-bonding interaction. We estimated the domain size of the aggregates using a comparison of the absorption saturation thresholds in aqueous solution to organic solvent THF and methanol and conclude that in water the size of the aggregate in saturated solution is at least 4. It is likely that Pchlide forms dimers in organic solvents like THF as well, resulting in the appearance of a new absorption band at 646 nm (see figure 6.2.B). In this case the red-shifted Q_Y absorption can be due to excitonic coupling provided either by direct stacking of adjacent parallel macrocycles or due to an orthogonally oriented dimer via a Mg---O=C coordination bond. Previously it was

shown[129] by quantum chemical calculations that various aggregate structures composed of chlorophyll a – dioxane tetramers can be responsible for the appearance of red-shifted Q_Y absorption bands.

The restoration of the emission intensity and the blue shift of the Q_Y band in Pchlide aqueous solution upon addition of THF or pyridine, see figure 6.2.C, can now be explained by the ligation of the central magnesium ion by a THF or pyridine molecule, which prevents coordination with a water molecule and breaks the Mg--(OH)--O=C coordinated Pchlide-water adduct states. We also showed that addition of extra OH^- into the Pchlide aqueous solution shifts the position of the Q_Y absorption further to the red (about 2 nm), confirming the correlation between H-bonding, coordination interactions and red shift of the visible absorption. The presence of an OH^- ion in the vicinity of the central magnesium and the keto group is a crucial factor determining the very complex excited state dynamics in neat water.

The coordinating internal water molecules, OH---H, possess acidic character due to the high mobility of the proton, making the C=O keto bond more likely to be protonated. The intensity loss of the C=O mode in the excited state (figure 6.7), may be the marker of a protonation of the C=O mode. As we argued above, the decay on the 0.5 and 5 ps time scale in the fluorescence and visible transient absorption spectra is due to loss of stimulated emission due to the formation of a CT state, rather than to a loss of excited states. The decay of the C=O mode can therefore not be explained by excited state decay alone: Assuming that the basic structural unit consists of 4 Pchlides, then exciting under saturating conditions should lead to a population of two of these, and to a loss of the initial signal amplitude after annihilation of a factor of two. Clearly, the decay we see in figure 6.7, though difficult to quantify, is significantly more. Generally speaking, the processes of site-specific solvation and protonation of the keto bond in the excited state can be directly related to formation of a state possessing a charge-transfer character. The possibilities of CTS formation through exciplex mechanism were discussed earlier[142], and tautomeric charge-transfer reactions were proposed by Fong[133, 143] in the study of chlorophyll water adduct states. Basically, the scheme involves the breaking of the internal coordinating water molecule resulting in ligation of Mg with an OH ion and protonation of the C=O keto group of the other chlorophyll, which can also be considered as the well known metal-to-ligand / ligand-to-metal charge-transfer state formation mechanism.

The possibility of mixing exciton states with CTS was suggested previously in a number of works, for example in red-most chlorophylls in large photosynthetic complexes like PS1[144], and in LHCa1-4 in PS1[145], and was experimentally demonstrated by Stark spectroscopy[146, 147] , also proposed by Wasielewski in fixed-distance chlorophyll-

porphyrin perpendicularly oriented heterodimers[148]. In the latter the compounds, which formed pure radical pairs, demonstrated the appearance of red 670-850 nm ESA signals only, whereas chlorophyll-porphyrin compounds with supposed CTS/S1 mixing in addition to it showed enhancement of nonradiative decay in TA and red shift of GS bleach with increasing solvent polarity.

In addition it has to be mentioned that there is a striking resemblance of kinetics found in Pchlide aqueous solution with other more complicated photosynthetic systems like Photosystem II core antenna complexes CP43[132] and CP47[67]. In both systems there was observed fast dramatic multi-exponential loss of initial signal with rates of about 1 ps and 10 ps in CP47, and with rates of about 200 fs, 3 ps, 12 ps in CP43. The final long-lived spectra are found to be red-shifted relatively to initial spectrum, and there was an enhancement of the blue side of Q_Y band in negative TA signals upon increase of excitation power as well.

6.5. Conclusions

Protochlorophyllide (Pchlide) is an important natural porphyrin. The biosynthesis of an entire photosynthetic apparatus in green plants depends on the light-driven redox reaction carried out by POR enzyme in which Pchlide is transformed into an immediate precursor of chlorophyll a. In plants, the oxidoreductase enzyme POR reduces protochlorophyllide into chlorophyllide, using NADPH as a cofactor. The reduction involves the transfer of two electrons and two protons to the C17=C18 double bond of Pchlide, and the reaction is initiated by the absorption of light by Pchlide itself[20, 52]. However the dominating and photoactive form of Pchide in the intact etiolated leafs is known to be the 655 nm form, actually resembling the red-shifted absorptions of Pchlide in aqueous solutions. The appearance of the 655 nm form *in vivo* was mainly assigned to formation of protein aggregates, either dimers or tetramers[4, 149-151] because of aggregation between POR complexes on etioplast membrane. For a detailed review of the POR *in vivo* studies we refer to Belayeva, Litvin[4]. However the role of the 655 nm *in vivo* form in the catalytic mechanism has remained unclear so far.

In this work we present the results of ultrafast time-resolved transient absorption and fluorescence experiments performed on protochlorophyllide in aqueous solution in the 480-720 nm visible region and in the 1780-1600 cm^{-1} mid-IR region.

We have shown that Pchlide dissolved in water forms aggregates in which excitonic interactions dominate the optical properties. We have demonstrated the population at high excitation density of multi-exciton manifolds, characterized by blue-shifted stimulated emission and red-shifted excited state absorption in comparison to those of the one-exciton

manifold. The relaxation dynamics of the multi-exciton manifolds into the one-exciton manifold occurs in ~10 ps. We suggest that this rate is slow, because of the formation of a charge-transfer state between the Pchlide molecule and its coordinating water molecule, making the exciton relaxation subject to charge recombination. Support for the charge-transfer process comes form the observed decrease in intensity of the C=O stretch mode in the excited state, concurrent with loss of stimulated emission, on a 0.5 and 5 ps time scale.

In order to explain the excited state dynamics in excitonically coupled Pchlide aggregates in more detail, we apply exciton theory (the exciton theory on the basis of one-, two-, three-, and four-exciton states with phenomenological Gaussian lineshape and static disorder) to model the time-resolved TA spectra in the next chapter.